ACS PHYSICAL CHEMISTRY Au
AN OPEN ACCESS JOURNAL OF THE AMERICAN CHEMICAL SOCIETY

pubs.acs.org/physchemau

Article

Equilibrium Thermodynamics of the Dimers and Trimers of H_2 and D_2 and Their Heterodimer $(H_2)(D_2)$

Arthur M. Halpern*

Cite This: *ACS Phys. Chem Au* 2022, 2, 346−352

Read Online

ACCESS | Metrics & More | Article Recommendations | Supporting Information

ABSTRACT: The equilibrium thermochemical properties of the dimers and trimers of H_2 and D_2 are obtained from the equations of state (EOSs) of normal H_2 and D_2. The standard dimer and trimer equilibrium constants K_D^o and K_T^o and $\Delta H_{D,T}^o$ and $\Delta S_{D,T}^o$ are reported for these weakly bound van der Waals molecules between 25 and 45 K. Statistical thermodynamics (ST) calculations of H_2 and D_2 dimerization using Morse pair potentials to account for intermolecular interactions, obtained from recent experimental work, are in qualitative agreement with the EOS results. The entropies of the H_2 and D_2 dimers and trimers are calculated from the EOS ΔS^o values and ST calculations of the monomer entropies.

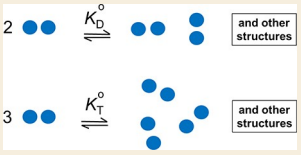

KEYWORDS: *equilibrium thermodynamics, statistical thermodynamics, van der Waals clusters, hydrogen dimer, deuterium dimer, hydrogen trimer, deuterium trimer, $(H_2)(D_2)$ heterodimer*

INTRODUCTION

The weak and subtle noncovalent interactions between atoms and molecules that give rise to the formation of dimers, trimers, higher-order *n*-mers, and larger clusters have been of particular interest for many years.[1−6] They have been the focus of numerous theoretical investigations into the nature of these weak associations, e.g., in the H_2 and D_2 dimers,[7−10] as well as the subject of an ab initio study of hydrogen molecular clusters.[11]

The use of mass spectrometry, in tandem with jet-cooled molecular beam methods, has led to the observation and characterization of such association pairs and aggregates.[12,13] For example, in 1964, Leckenby et al. reported the presence of "condensation embryos" accompanying the isentropic expansion of a gas into a vacuum chamber.[1] The binding mechanism of these species was characterized as "van der Waals forces", giving rise to the appellation "van der Waals molecules" to such species.

In 1964, Watanabe and Welsh reported the presence of "$(H_2)_2$ complexes" from increases in the collision-induced infrared absorption spectra of H_2 vapor and suggested a dissociation energy of 5.0 K and an intermolecular separation of 4.2−4.6 Å.[14] They also provided evidence of two bound states and assigned features of the spectra to the presence of bound and metastable rotational states. Subsequent studies reported the existence and properties of the D_2 dimer.[15,16]

Of the diverse array of van der Waals dimers formed from atoms and molecules, the weakest, not surprisingly, are those containing few electrons, e.g., He, H_2, and Ne, with Lennard-Jones well depths (obtained from the second virial coefficients) of 10.22, 37.00, and 35.60 K, respectively.[17]

The present work focuses on the equilibrium thermodynamic properties of the dimers and trimers of H_2 and D_2 obtained from their equations of state (EOSs) and is a continuation of previous studies relating to the rare gases He,[18] Ne to Xe,[19] and the small molecules CH_4 and CO_2.[20] A similar approach was previously employed by Ruscic to water dimerization.[21]

Since H_2 is emerging as an important alternative to fossil fuels,[22] although it might play a small role in global warming,[23] it is important to have data relating to the equilibrium thermodynamics of dimer and trimer formation.

COMPUTATIONAL METHODS

The standard dimer and trimer equilibrium constants are expressed as

$$2\mathrm{M} \rightleftharpoons \mathrm{D} \quad (K_D^o) \tag{1}$$

and

$$3\mathrm{M} \rightleftharpoons \mathrm{T} \quad (K_T^o) \tag{2}$$

where

$$K_D^o = \frac{P_D/P^o}{(P_M/P^o)^2} = \left(\frac{P_D}{P_M^2}\right)(P^o) \tag{3}$$

and

$$K_T^o = \frac{P_T/P^o}{(P_M/P^o)^3} = \left(\frac{P_T}{P_M^3}\right)(P^o)^2 \tag{4}$$

in which P_M, P_D, P_T, and P^o are the equilibrium partial pressures, in bars, of the monomer, dimer, trimer and total pressure, and the standard pressure (1 bar), respectively. It follows from eqs 1 and 2 that the equilibrium constant for M + D ⇌ T is K_T^o/K_D^o.

Received: March 13, 2022
Revised: April 1, 2022
Accepted: April 4, 2022
Published: April 13, 2022

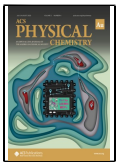

Table 1. Standard Thermochemical Properties of H_2 and D_2 Dimerization between 25 and 45 K

	H_2-H_2			D_2-D_2		
T (K)	K_D^o	ΔH_D^o (J/mol)	ΔS_D^o (J/(mol-K))	K_D^o	ΔH_D^o (J/mol)	ΔS_D^o (J/(mol-K))
25	0.051236(2)	−511.96(3)	−45.183(1)	0.060529(2)	−535.04(3)	−44.721(1)
27	0.042304(2)	−563.85(3)	−47.181(1)	0.049603(2)	−582.10(3)	−46.533(1)
29	0.035314(1)	−614.67(3)	−48.995(1)	0.041217(1)	−627.01(4)	−48.135(1)
31	0.029761(1)	−666.82(4)	−50.732(1)	0.034650(1)	−673.57(4)	−49.685(1)
33	0.025290(1)	−720.41(4)	−52.406(1)	0.029417(1)	−721.97(4)	−51.196(1)
35	0.021647(1)	−775.65(5)	−54.030(1)	0.025186(1)	−772.40(5)	−52.678(1)
37	0.018648(1)	−832.70(5)	−55.614(1)	0.021719(1)	−824.95(5)	−54.137(1)
39	0.016155(1)	−891.74(6)	−57.167(1)	0.018847(1)	−879.71(6)	−55.577(2)
41	0.0140644(5)	−953.08(6)	−58.700(2)	0.018847(1)	−936.87(7)	−57.005(2)
43	0.0122979(4)	−1016.9(7)	−60.219(2)	0.0144141(5)	−996.49(7)	−58.424(2)
45	0.0107945(3)	−1081.5(7)	−61.686(2)	0.0126871(4)	−1056.6(8)	−59.790(2)

The details of the method used to obtain the standard equilibrium constants and values of ΔH^o and ΔS^o for dimerization and trimerization have been described in previous work and are also presented in the Supporting Information. Briefly, the EOS of the gas is used to obtain the compression factor, Z (i.e., PV_m/RT), over a certain temperature range. It is demonstrated in ref 19 (and shown in the Supporting Information) that Z is related to the mole fractions of the monomer, dimer, and trimer through its reciprocal, r, viz.

$$r \equiv \frac{1}{Z} \cong x_M + 2x_D + 3x_T \tag{5}$$

It should be noted that the model assumes the presence of only monomers, dimers, and trimers. The gas pressures used in the calculations, at each temperature, are chosen to be low enough to assume the validity of eq 5. The key equation used to obtain $K_D^o$and K_T^o at each temperature is

$$(r-1) = K_D^o(x_M^2 P) + K_T^o(2x_M^3 P^2) \tag{6}$$

where P is the total pressure. K_D^o and K_T^o are obtained from a multiple regression analysis of eq 6 over a certain pressure range. Since the values of x_M are needed over that pressure range, the initial values of $K_D^o$and K_T^o are first obtained and then used to calculate $x_M(P)$. These initial values are obtained from a regression of

$$\frac{(r-1)}{(2-r)^2} \simeq K_D^o P + 2K_T^o P^2 \tag{7}$$

These initial values of K_D^o and K_T^o are used to calculate x_M in eq 6, which is employed to obtain the more precise ones that furnish the data reported here. The derivation of eq 7 can be found in the Supporting Information. It should be noted that these initial values of K_D^o and K_T^o are very close to those produced from eq 6 because the pressure ranges used are low enough to ensure that x_D and x_T are sufficiently small.

The calculations reported here are based on the EOSs of H_2 and D_2 developed by Leachman et al.[24] and Richardson et al.,[25] respectively, and implemented in the PC application miniREFPROP.[26] The temperature range used in this study is 25−45 K, and the pressure ranges at each temperature were chosen to keep the monomer mole fraction between 0.9940 and 0.9970. This measure keeps x_D and x_T from being too large below 25 K and too small above 45 K, which would affect the precision of K_D^o and K_T^o in the regression of eq 6. The pressure ranges used in the H_2 and D_2 calculations range from 0.0580 to 0.274 and 0.0500 to 0.234 bar, respectively. The largest mole fractions of the dimer and trimer for both H_2 and D_2 are roughly constant over the temperature range used, i.e., with $x_{D,max}$ about 6×10^{-3} and $x_{T,max}$ between 6×10^{-5} and 7×10^{-5}. Detailed information about the pressure ranges used in the H_2 and D_2 calculations and the corresponding dimer and trimer mole fractions is shown in the Supporting Information.

From the K_D^o and K_T^o, values of the thermodynamic quantities ΔH^o, ΔG^o, and ΔS^o were obtained from the relations

$$\Delta H^o = RT^2 \frac{\mathrm{d}\ln K^o}{\mathrm{d}T} \tag{8}$$

$$\Delta G^o = -RT \ln K^o \tag{9}$$

and

$$\Delta S^o = \frac{\Delta H^o - \Delta G^o}{T} \tag{10}$$

RESULTS AND DISCUSSION

Hydrogen and Deuterium Monomer-Dimer Equilibrium: EOS-Based Calculations

Table 1 contains values of K_D^o, ΔH_D^o, and ΔS_D^o for both H_2 and D_2 dimerization between 25 and 45 K for the EOS-based calculations. The standard deviation of regression of the fits to eq 6 ranged between 8.9×10^{-8} at 25 K and 7.4×10^{-8} at 45 K for H_2 and 8.5×10^{-8} to 7.7×10^{-8} for D_2. These results, for 1 K intervals, are available in the Supporting Information. Statistical thermodynamics calculations of these quantities for H_2 and D_2 dimerization using a Morse potential to describe H_2 and D_2 intermolecular interactions are presented later.

The results show that, as expected, K_D^o for the D_2 dimer is larger than that for H_2 and ΔH_D^o is more negative because of the smaller zero point energy (larger zero point dissociation energy D_0). The values of ΔS_D^o can be used to obtain the dimer entropy S_D^o through the relationship

$$\Delta S_D^o = S_D^o - 2S_M^o \tag{11}$$

where S_M^o is the entropy of the monomer, H_2 or D_2. The latter is calculated from the respective molecular rotational constants (vibrational contributions are negligible in the temperature range used because of the high vibrational frequencies). However, care must be taken to account for the ortho-para nuclear spin isomers of H_2 and D_2. To comport with the EOSs employed,[24,25] the calculations used to obtain S_M^o are for "normal" hydrogen and deuterium, in which the populations of the ortho and para forms are constrained to the ratio of the respective nuclear spin function degeneracies, i.e., 3:1 for H_2 and 6:3 for D_2, independent of temperature. The calculations of the normal H_2 and D_2 partition functions follow the methods of Colonna et al.[27] and Le Roy et al.[28] The results are available in the Supporting Information, along with the respective S_M^o values and are in excellent agreement with those reported in ref 28. Table 2 contains S_D^o, obtained from eq 11.

https://doi.org/10.1021/acsphyschemau.2c00015
ACS Phys. Chem Au 2022, 2, 346−352

Table 2. Values of the Monomer and Dimer Entropies of H_2 and D_2 and Their Translational and Rotational Entropies between 25 and 45 K[a]

	H_2		D_2	
T (K)	S^o_M	S^o_D[b]	S^o_M	S^o_D
25	72.93	100.67	77.76	110.80
27	74.53	101.87	79.37	112.20
29	76.01	103.03	80.86	113.58
31	77.40	104.06	82.26	114.83
33	78.70	104.99	83.58	115.96
35	79.92	105.81	84.83	116.98
37	81.08	106.54	86.02	117.90
39	82.17	107.17	87.15	118.73
41	83.21	107.72	88.24	119.48
43	84.20	108.18	89.29	120.17
45	85.15	108.60	90.31	120.83

[a]Entropies in J/(mol-K). [b]Calculated from eq 11.

Hydrogen and Deuterium Monomer-Dimer Equilibrium: Statistical Thermodynamics Calculations

To provide corroboration of the EOS-based results presented in Table 1, statistical thermodynamics (ST) calculations were carried out to obtain independently these thermochemical quantities. The recent publication of Khan et al.[29] presents a propitious opportunity to carry out such calculations. It reports the results of femtosecond laser-induced Coulomb explosion imaging experiments that permit a statistical sampling to be made of the intermonomer distribution function (the square of the wavefunction) of single-molecular dimers of H_2, D_2, and their heterodimer $(H_2)(D_2)$. From this work, the authors obtained centrosymmetric potential energy functions that essentially represent the projection of the full six-dimensional potential energy surfaces of the dimers onto a one-dimensional PE coordinate—the intermolecular distance. Thus, they reported the parameters of the Morse, Lennard-Jones, and the modified Buckingham potentials. Such one-dimensional centrosymmetric potentials are consistent with the description of the monomer−monomer interactions that lead to gas imperfection expressed by the EOS since the latter reflects the array of intermolecular interactions under equilibrium conditions.

For the ST calculations reported in the present study, the Morse potential is used to obtain the dimer rovibrational energies employed in the calculation of the dimer partition functions. The intermolecular potential used is

$$V(R) = D_e\{1 + \exp[-2\alpha(R - R_e)] - 2\exp[-\alpha(R - R_e)]\} + \frac{\hbar^2}{2\mu R^2}J(J+1) \quad (12)$$

in which R is the intermonomer separation. The first term is the Morse function, where D_e is the well depth, R_e is the value of R at the potential minimum (of the rotationless dimer), and α is a parameter that affects the curvature of the bottom of the well.[30] The second term accounts for the rotational energy of the dimer, in which $\hbar$ is the Planck constant divided by 2π, μ is the reduced mass, and J is the rotational quantum number.[30] The Morse potential parameters are shown in Table 3.

The eigenvalues and eigenfunctions of the Schrödinger equation with potential function (eq 12) were obtained using a finite difference method for chosen values of J.[31] The rotational term in eq 12 produces (for $J \neq 0$) a rotational barrier to dissociation.[30] Figure 1 shows plots of the potential function of eq 12 along with the square of the wavefunction, $\Psi^2_J(R)$, of the dimers.

Table 3. Morse Parameters Used in the ST Calculations[a]

dimer	D_e (K)	R_e (Å)	α (Å^{-1})[b]
H_2−H_2	43(2)	3.50(2)	1.80
D_2−D_2	46(3)	3.49(3)	2.02
H_2−D_2	49(6)	3.47(5)	1.97

[a]Values of D_e and R_e are from ref 29 (the reported uncertainties are shown). [b]Values of α are obtained from a regression fit of the Morse curves shown in Figure S3 of the supporting information of ref 29 to the first term on the RHS of eq 12 using values of D_e and R_e provided in ref 29 and shown in Table 3.

These graphs illustrate the extent to which Ψ^2_J extends to larger values of R, indicating the quantum mechanical tunneling that arises from the small well depths and reduced masses. As expected, Ψ^2_J for H_2−H_2 extents farther out than it does for D_2−D_2. Panel (d) shows the rotational barrier (arising from the second term of the RHS of eq 12), which is about 8 K. The finite difference results show for all dimers only one vibrational level, the zero point state. Tunneling is appreciable for the rotational excited levels.

Table 4 contains the eigenvalues of the relevant J levels of the dimers along with the percentage tunneling into the nonclassical ranges of R, i.e., values of R for which $V(R)_J > E_J$.

The zero point dissociation energies of the dimers, $D_0 = D_e - E_{J=0}$, where D_e is from ref 29 and $E_{J=0}$ is from the calculations in Table 4, are 4.4, 11, and 7.9 K, in excellent agreement with the values in ref 29 and also with those calculated from the analytical solution of the Morse potential.[32] It can be seen that the energies of the J = 3, 4, and 3 states of dimers lie above the respective D_e levels and have ∼100% probabilities that the intermonomer separations are consistent with dissociation. The dimer rotational partition functions are calculated using the J = 0−2 states of $(H_2)_2$ and H_2D_2 and the J = 0−3 states for $(D_2)_2$. It should be noted, however, that the energy of the J = 2 state of $(H_2)_2$ is close to the top of the rotational barrier (ca. 1.6 K), and therefore (along with the small reduced mass of this dimer), a large fraction of the intermonomer distribution probability is in the nonclassical region (ca. 83%). This is likely an artifact caused by the characteristics of the Morse function since adjustment of the potential parameters, within the uncertainties indicated in ref 29, produces a more strongly bound J = 2 level that justifies its inclusion in the calculation of the rotational partition function. It should be noted that both the LJ and modified Buckingham potentials of ref 29 produce larger D_0 values, i.e., 5.8 and 5.4 K, respectively (c.f. 4.4 K for the Morse potential), and, accordingly, fully bound J = 2 states.

The Morse potential calculations are given credence by the experimental findings of Watanabe and Welsh,[14] who estimated the H_2−H_2 dimer binding energy to be ∼5.0 K, which compares with 4.4 K, from the results in Table 4 and from ref 29. They[14] assigned dimer rotational transition energies of 2.7 and 6.9 K, in qualitative agreement with 2.3 and 5.9 K for J = 0−1 and J = 0−2 transitions, respectively (Table 4).

Statistical Thermodynamics Calculations

The standard equilibrium constant K^o_D for the H_2 and D_2 dimers was calculated from

https://doi.org/10.1021/acsphyschemau.2c00015
ACS Phys. Chem Au 2022, 2, 346−352

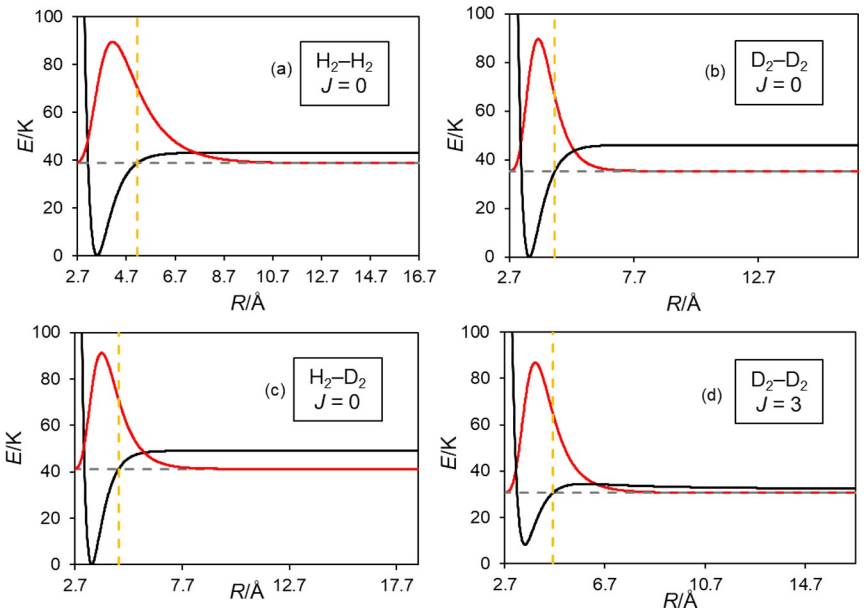

Figure 1. Plots of the potential energy function $V(R)$ in eq 12 (black) and the distribution function Ψ_J^2 (red) for the $(H_2)_2$, $(D_2)_2$, and H_2−D_2 dimers. The horizontal black dashed lines correspond to the eigenvalues E_J, and the vertical yellow dashed lines indicate values of R for which $V(R) = E_J$. (a) H_2 dimer, $J = 0$; (b) D_2 dimer, $J = 0$; (c) H_2−D_2 heterodimer, $J = 0$; (d) D_2 dimer, $J = 3$. The distribution functions are arbitrarily scaled and are vertically shifted to converge to the respective eigenvalues (horizontal dashed black lines).

Table 4. Eigenvalues of eq 12 Corresponding to the Different J Levels of the Dimers and the Percentage Tunneling[a]

	H_2−H_2			D_2−D_2			H_2−D_2		
D_e[b]	43			46			49		
J	E_J[c]	V_{barr}[d]	% nc[e]	E_J[c]	V_{barr}[d]	% nc[e]	E_J[c]	V_{barr}[d]	% nc[e]
0	38.6		32.8	35.4		24.3	41.1		28.3
1	40.9	2.9	37.1	36.8	9.6	24.8	43.3	6.3	30.0
2	44.5	1.6	82.8	39.7	7.8	26.4	47.2	4.2	35.1
3	45.6		99.8	44.0	5.5	29.7	50.9		98.8
4				48.2		98.9			

[a]Energies are in K. [b]D_e values from ref 29 (see also Table 2). [c]Obtained from finite difference calculations.[31] [d]Rotational barrier $[V(R)_J]_{max} - E_J$. [e]Percent tunneling into the nonclassical region.

$$K_D^o = \frac{10^5 \Lambda_M^6 q_{D,rot\text{-}vib}}{kT \Lambda_D^3 q_{M,rot\text{-}vib}^2} \exp(D_0/T) \tag{13}$$

in which

$$\Lambda_{M,D} = \frac{h}{(2\pi m_{M,D} kT)^{1/2}} \tag{14}$$

comes from the standard translational partition functions of the monomer and dimer, $m_{M,D}$ is the respective molecular mass, D_0 is the dissociation of the dimer (from the zero point level), in K, and h and k are the Planck and Boltzmann constants, respectively. The factor of 10^5 indicates the standard pressure (in bars).

In eq 13, $q_{Mrot\text{-}vib}$ and $q_{Drot\text{-}vib}$ are the monomer and dimer rotational-vibrational partition functions, respectively. Because of the high stretching frequencies of H_2 and D_2, the vibrational contribution to the internal energy of the monomers is negligible at the low temperatures used in the EOS calculations. Thus, only rotational states need to be considered in calculating the monomer partition functions. These values are obtained from a discrete sum over states, taking into account nuclear spin statistics of the ortho and para forms, as appropriate.[27,28] The results of these calculations are available in the Supporting Information.

Calculations of $q_{Drot\text{-}vib}$ are challenging. Not only is there a distribution of dimer structures, but they consist of a mixture of ortho-ortho, para-para, and ortho-para nuclear spin isomers. In addition, the dimers are expected to have four low frequency intermonomer vibrational modes, which would be populated at the temperatures in this study, while the two high frequency modes associated with the perturbed H−H (D−D in the D_2 dimer) stretching mode would be scantly populated. While ab initio calculations can provide values of the six harmonic frequencies and the rotational constants, it is not clear the extent to which these rovibrational levels actually contribute to the partition function because of the shallowness of the potential wells and the high zero point energies relative to the well depths, i.e., small D_0 values.

However, by collapsing the six-dimensional PE surface of the dimer into a one-dimensional centrosymmetric one (e.g., the Morse potential), as is accomplished in the work of Khan et al.,[29] the opportunity arises to calculate $q_{Drot\text{-}vib}$ since, in this model, there is only one vibrational mode, the van der Waals stretch, thus considerably simplifying the calculation. The rotational energy levels shown in Table 4 are used to calculate q_{Drot}.

https://doi.org/10.1021/acsphyschemau.2c00015
ACS Phys. Chem Au 2022, 2, 346−352

Table 5. Calculated Thermochemical Properties Related to the Dimerization of H_2 and D_2 between 25 and 45 K[a]

	H_2-H_2			D_2-D_2			H_2-D_2		
T (K)	K_D°	ΔH_D° [b,c]	ΔS_D° [d,e]	K_D°	[b,c]	ΔS_D° [d,e]	K_D°	ΔH_D° [b,c]	ΔS_D° [d,e]
25	0.0430	−522	−47.1	0.0836	−567	−43.3	0.0716	−551	−43.9
27	0.0354	−567	−48.8	0.0677	−612	−45.1	0.0584	−596	−45.7
29	0.0296	−608	−50.2	0.0558	−654	−46.5	0.0483	−637	−47.2
31	0.0250	−649	−51.6	0.0466	−696	−48.0	0.0406	−679	−48.6
33	0.0214	−691	−52.9	0.0394	−739	−49.3	0.0344	−721	−49.9
35	0.0184	−732	−54.1	0.0336	−782	−50.5	0.0295	−763	−51.1
37	0.0160	−774	−55.3	0.0290	−826	−51.8	0.0255	−806	−52.3
39	0.0140	−815	−56.4	0.0251	−870	−52.9	0.0222	−849	−53.4
41	0.0124	−857	−57.4	0.0220	−916	−54.1	0.0195	−893	−54.5
43	0.0110	−898	−58.4	0.0193	−962	−55.2	0.0172	−937	−55.6
45	0.00980	−938	−59.3	0.0171	−1007	−56.2	0.0153	−979	−56.5

[a] K_D° calculated from eq 12. [b] J/mol. [c] Calculated from eq 8. [d] J/(mol-K). [e] Calculated from eqs 9 and 10.

Table 6. Standard Thermochemical Properties of H_2 and D_2 Trimerization between 25 and 45 K

	K_T°		ΔH_T° (J/mol)		ΔS_T° (J/(mol-K))	
T (K)	H_2	D_2	H_2	D_2	H_2	D_2
25	$5.171(1) \times 10^{-3}$	$7.375(1) \times 10^{-3}$	−1057(1)	−1094(1)	−86.07(6)	−84.58(5)
27	$3.4842(7) \times 10^{-3}$	$4.9069(9) \times 10^{-3}$	−1158(2)	−1192(2)	−89.96(6)	−88.37(6)
29	$2.4071(5) \times 10^{-3}$	$3.3553(6) \times 10^{-3}$	−1258(2)	−1287(2)	−93.52(7)	−91.77(6)
31	$1.696(3) \times 10^{-3}$	$2.3487(4) \times 10^{-3}$	−1363(2)	−1387(2)	−97.02(7)	−95.08(7)
33	$1.2160(2) \times 10^{-3}$	$1.6757(3) \times 10^{-3}$	−1474(2)	−1492(2)	−100.47(7)	−98.34(7)
35	$8.845(2) \times 10^{-4}$	$1.2150(2) \times 10^{-3}$	−1587(3)	−1601(3)	−103.81(7)	−101.55(8)
37	$6.518(1) \times 10^{-4}$	$8.935(2) \times 10^{-4}$	−1706(3)	−1716(3)	−107.11(8)	−104.76(8)
39	$4.8560(9) \times 10^{-4}$	$6.646(1) \times 10^{-4}$	−1833(3)	−1840(3)	−110.43(8)	−108.02(9)
41	$3.6505(7) \times 10^{-4}$	$4.9922(9) \times 10^{-4}$	−1965(4)	−1970(4)	−113.74(9)	−111.26(9)
43	$2.7669(5) \times 10^{-4}$	$3.7816(7) \times 10^{-4}$	−2107(4)	−2110(4)	−117.12(9)	−114.59(9)
45	$2.1098(4) \times 10^{-4}$	$2.8829(5) \times 10^{-4}$	−2257(4)	−2257(4)	−120.53(9)	−117.9(1)

Equation 13 is used to calculate K_D°, ΔH_D°, and ΔS_D° of the three dimer systems. These results are shown in Table 5. Because of the uncertainty in these calculations, the results may be considered qualitative and are reported to more significant figures than perhaps warranted to allow comparisons to be made with the EOS results. In calculating the properties of the heterodimer equilibrium, $q^2_{M,\,rot\,-\,vib}$ in eq 13 is replaced by $q_{H_2rot\,-\,vib}q_{D_2rot\,-\,vib}$.

These ST results in Table 5 are in good qualitative agreement with the EOS results in Table 1. A closer comparison can be made by obtaining the dimer entropies $S^\circ_{D,\,tot}$ from the ST-calculated values of ΔS_D° (Table 5) using eq 11 and the monomer entropies listed in Table 2. These calculations produce values that range from 98.8 to 111 J/mol-K for the H_2 dimer and 112 to 124 J/(mol-K) for the D_2 dimer between 25 and 45 K, in satisfactory comparison with 101−109 J/(mol-K) and 111−121 J/(mol-K), respectively.

Hydrogen and Deuterium Monomer-Trimer Equilibrium: EOS Calculations

In this section, the trimer equilibrium (eq 2) involving H_2 and D_2 as monomers is considered. The EOS-based results (eqs 6 and 8−10) are summarized in Table 6. It should be noted that, in these calculations, the pressures were low enough to keep the trimer mole fractions reasonably small. They ranged from 1.6×10^{-5} to 7.1×10^{-5} for both H_2 and D_2.

From these results, we see that, as expected, for both H_2 and D_2, the values of K_T° are smaller than those of K_D° and that the trimerization enthalpy and entropy changes are more negative than those for dimerization (see Table 1). Moreover, both ΔH_T° and ΔS_T° values are about twice those of the respective values for dimerization at each temperature and their regression uncertainties are, as would be anticipated, larger than those for dimerization. The uncertainties in K_T° are about 0.1 (at 25 K) and 0.02 (at 45 K) that of K_D°.

It might be expected that, for these weakly bound van der Waals dimers and trimers, ΔH_T° would be about 3 times larger than ΔH_D° (the trimer being held together by three "van der Waals" bonds as compared with two for the dimer). In fact, the ratio of well depths (D_e), obtained from the counterpoise-corrected MP2/aug-cc-pVTZ calculations reported by Carmichael et al., is about 3.0.[11] This ratio is based on the equilibrium structures of the T-shaped dimer and cyclic planar C_{3h} structure.[11] However, the situation regarding enthalpy changes is more complicated. For example, from energy balance considerations

$$\Delta H_D = -D_{0,D} + U_{D,int} - 2U_{M,int} - {}^5/_2 RT \quad (15)$$

and

$$\Delta H_T = -D_{0,T} + U_{T,int} - 3U_{M,int} - 5RT \quad (16)$$

where $D_{0,D}$ and $D_{0,T}$ are the respective zero point dissociation energies of the dimer and trimer, and the U terms are the corresponding internal energies of the dimer, monomer, and trimer.

As noted above, the potential energy surface of the H_2 dimer is shallow and contains several minima, with low barriers separating them. Moreover, the zero point vibrational energies of the different H_2 dimer species are larger than or comparable

https://doi.org/10.1021/acsphyschemau.2c00015
ACS Phys. Chem Au 2022, 2, 346−352

with the local well depths. That is why the reduction of the six-dimensional surface of the dimer into a one-dimensional one[29] is so useful since it allows calculations, however simplified, to be carried out on the dimer properties.

The case of the trimer is all the more fraught with such complications, making ST calculations of the trimer infeasible. Although the trimer potential well is about 3 times the depth as the monomer for specific dimer and trimer structures, the combined zero point energy of the nine low frequency modes becomes comparable with the well depth itself. Thus, ab initio calculations taking into account the anharmonic dimer and trimer vibrational energies produce small D_0 values, i.e., 0.82−2.3 K for the H_2 monomer and 3.0−3.2 K for the trimer.[11] These compare with D_e values of 39.6 and 121 K, respectively.[11]

The empirical entropies of the H_2 and D_2 trimers can be found using the same method as for the dimers, i.e., $S^\circ_T = \Delta S^\circ_T + 3S^\circ_M$, where ΔS°_T is obtained from the EOS calculations. The results are shown in Table 7, which also contains the trimer internal entropies, obtained by subtracting the translational entropy from S°_T.

Table 7. Translational, Rotational, and Total Entropies of the H_2 and D_2 Trimers between 25 and 45 K[a]

	H_2		D_2	
T (K)	S°_M	S°_T[b]	S°_M	S°_T[b]
25	72.93	132.7	77.76	148.7
27	74.53	133.6	79.37	149.7
29	76.01	134.5	80.86	150.8
31	77.40	135.2	82.26	151.7
33	78.70	135.6	83.58	152.4
35	79.92	136.0	84.83	152.9
37	81.08	136.1	86.02	153.3
39	82.17	136.1	87.15	153.4
41	83.21	135.9	88.24	153.5
43	84.20	135.5	89.29	153.3
45	85.15	134.9	90.31	153.0

[a]Entropies in J/(mol-K). [b]Calculated from $\Delta S^\circ_T = S^\circ_T - 3S^\circ_M$.

The H_2 trimer internal entropies (presumably largely due to rotational states) are larger than those of the dimer by a factor of ca. 2.0, while for the D_2 trimer, they are ca. 2.5 those of the dimer, reflecting the larger number of such states in the trimers vis-à-vis the dimers. It is also seen that, as in the case of the dimers (Table 2), the trimer internal entropies decrease with temperature.

CONCLUSIONS

Equations of state have been used to obtain the equilibrium thermochemical properties and the entropies of the weakly bound van der Waals H_2 and D_2 dimers and trimers of H_2 and D_2 between 25 and 45 K. The dimer results are supported by statistical thermodynamics calculations based on a Morse potential, obtained from experimental studies.

ASSOCIATED CONTENT

Supporting Information

The Supporting Information is available free of charge at https://pubs.acs.org/doi/10.1021/acsphyschemau.2c00015.

Summary of the EOS computational method, tables of minimum and maximum pressures and dimer and trimer mole fractions, expanded tables of dimerization properties of H_2 and D_2, rotational and total entropies of H_2 and D_2, and analytical solution of the Morse function (PDF)

AUTHOR INFORMATION

Corresponding Author

Arthur M. Halpern − *Department of Chemistry and Physics, Indiana State University, Terre Haute, Indiana 47809, United States;* orcid.org/0000-0002-2211-2826; Email: arthur.halpern@indstate.edu

Complete contact information is available at: https://pubs.acs.org/10.1021/acsphyschemau.2c00015

Notes

The author declares no competing financial interest.

REFERENCES

(1) Leckenby, R. E.; Robbins, E. J.; Trevalion, P. A. Condensation embryos in an expanding gas beam. *Proc. Roy. Soc. Chem. Ser. A.* **1964**, *280*, 409−429.
(2) Ewing, G. E. Intermolecular interactions. Van der Waals molecules. *Angew. Chem. Int. Ed. Engl.* **1972**, *11*, 486−495.
(3) Novick, S. E.; Davies, P. B.; Dyke, T. R.; Klemperer, W. Polarity of van der Waals Molecules. *J. Am. Chem. Soc.* **1973**, *95*, 8547−8550.
(4) Ewing, G. E. Structure and Properties of van der Waals Molecules. *Acc. Chem. Res.* **1973**, *8*, 185−192.
(5) Blaney, B. L.; Ewing, G. E. van der Waals Molecules. *Annu. Rev. Phys. Chem.* **1976**, *27*, 553−584.
(6) Stogryn, D. E.; Hirschfelder, J. O. Contribution of Bound, Metastable, and Free Molecules to the Second Virial Coefficient and Some Properties of Double Molecules. *J. Chem. Phys.* **1959**, *31*, 1531−1545.
(7) Danby, G.; Flower, D. R. Theoretical Studies of van der Waals Molecules: the H_2-H_2 Dimer. *J. Phys. B: At. Mol. Phys.* **1983**, *16*, 3411−3422.
(8) Danby, G. Theoretical Studies of van der Waals Molecules: the D_2-D_2 Dimer. *J. Phys. B: At., Mol. Opt. Phys.* **1989**, *22*, 1785−1807.
(9) Hinde, R. J. A six-dimensional potential H_2—H_2 potential energy surface for bound state spectroscopy. *J. Chem. Phys.* **2008**, *128*, 154308.
(10) Patkowski, K.; Cencek, W.; Jankowski, P.; Szalewicz, K.; Mehl, J. B.; Garberoglio, G.; Harvey, A. H. Potential energy surface for interactions between two hydrogen molecules. *J. Chem. Phys.* **2008**, *129*, No. 094304.
(11) Carmichael, M.; Chenowith, K.; Dykstra, C. E. Hydrogen Molecule Clusters. *J. Phys. Chem. A* **2004**, *108*, 3143−3152.
(12) Henkes, W. Mass-spectrometric investigations of condensed rays of hydrogen. *Zeit. Naturforsch.* **1962**, *17a*, 786−789.
(13) Greene, F. T.; Milne, T. A. Mass spectrometric detection of polymers in supersonic molecular beams. *J. Chem. Phys.* **1963**, *39*, 3150−3151.
(14) Watanabe, A.; Welsh, H. L. Direct spectroscopic evidence of bound states of $(H_2)_2$ complexes at low temperatures. *Phys. Rev. Lett.* **1964**, *13*, 810−812.
(15) Watanabe, A.; Welsh, H. L. Pressure-induced infrared absorption of gaseous hydrogen and deuterium at low temperatures. I. The integrated absorption coefficients. *Can. J. Phys.* **1965**, *43*, 818−828.
(16) McKellar, A. R. W.; Welsh, H. L. Spectra of dimeric molecular hydrogen, dimeric molecular deuterium, and molecular hydrogen-molecular deuterium Van der Waals complexes. *Can. J. Phys.* **1974**, *52*, 1082−1089.
(17) Hirschfelder, J. O.; Curtiss, C. F.; Bird, R. B. *Molecular Theory of Gases and Liquids*; John Wiley: New York, 1954; p. 1110.
(18) Halpern, A. M. Thermodynamics of the Helium-4 Dimerization and Trimerization. *J. Phys. Chem. A.* **2021**, *125*, 9071−9076.
(19) Halpern, A. M. Equilibrium State Thermodynamic Properties of Rare Gas Dimers and Trimers Obtained From Equations of State and

Statistical Thermodynamics: Application to Neon, Argon, Krypton and Xenon. *J. Chem. Thermodyn.* **2021**, *162*, 106558.
(20) Halpern, A. M. The Thermodynamics of the van der Waals Dimer and Trimer Formation in Gaseous Carbon Dioxide and Methane and Their Heterodimers. *J. Chem. Thermodyn.* submitted for publication.
(21) Ruscic, B. Active Thermochemical Tables: Water and Water Dimer. *J. Phys. Chem. A* **2013**, *117*, 11940−11953.
(22) U. S. Department of Energy *Alternative Fuels Data Center, Hydrogen Basics* https://afdc.energy.gov/fuels/hydrogen_basics.html (accessed March, 2022).
(23) Derwent, R. G. *Hydrogen for Heating: Atmospheric Impacts. A literature review. BEIS Research Paper Number 2018: no. 21. Department for Business Energy and Industrial Strategy* https://assets.publishing.service.gov.uk/government/uploads/system/uploads/attachment_data/file/760538/Hydrogen_atmospheric_impact_report.pdf (accessed March, 2022).
(24) Leachman, J. W.; Jacobsen, R. T.; Penoncello, S. G.; Lemmon, E. W. Fundamental Equations of State for Parahydrogen, Normal Hydrogen, and Orthohydrogen. *J. Phys. Chem. Ref. Data* **2009**, *38*, 721−748.
(25) Richardson, I. A.; Leachman, J. W.; Lemmon, E. W. Fundamental Equation of State for Deuterium. *J. Phys. Chem. Ref. Data* **2014**, *43*, No. 013103.
(26) Lemmon, E. W.; Bell, I. H.; Huber, M. J.; McLinden, M. G.; miniREFPROP *An abbreviated version of NIST REFPROP. NIST Standard Reference Database 23, Version 95, DLL version 10.0.* https://trc.nist.gov/refprop/MINIREF/MINIREF.HTM (accessed March, 2022).
(27) Colonna, G.; D'Angola, A.; Capitelli, M. Statistical thermodynamic description of H_2 molecules in normal ortho/para mixture. *Int. J. Hydrogen Energy* **2012**, *37*, 9656−9668.
(28) Le Roy, R. J.; Chapman, S. G.; McCourt, F. R. W. Accurate Thermodynamic Properties of the Six Isotopomers of Diatomic Hydrogen. *J. Phys. Chem.* **1990**, *94*, 923−929.
(29) Khan, A.; Jahnke, T.; Zeller, S.; Trinter, F.; Schöffler, M.; Schmidt, L. Ph. H.; Dörner, R.; Kunitski, M. Visualizing the geometry of hydrogen dimers. *J. Phys. Chem. Lett.* **2020**, *11*, 2457−2463.
(30) Herzberg, G. *Molecular Spectra and Molecular Structure I. Spectra of Diatomic Molecules*; D. van Nostrand Company, Inc.: Princeton, N.J., 1950, pp. 425−430.
(31) *FINDIF: Finite Differences A graphical tool for analyzing one-dimensional potentials*. https://carbon.indstate.edu/FINDIF (accessed March, 2022).
(32) Matsumoto, A. Parameters of the Morse potential from second virial coefficients of gases. *Z. Naturforsch., A* **1987**, *42a*, 447−450.

https://doi.org/10.1021/acsphyschemau.2c00015
ACS Phys. Chem Au 2022, 2, 346−352